OPTIMIZATION OF FIXED BED WATER-GAS SHIFT CONVERTER FOR PRODUCTION OF PIPELINE GAS

C. Y. Wen and H. N. Kim

Department of Chemical Engineering
West Virginia University
Morgantown, West Virginia

1. INTRODUCTION

With the growing shortage of natural gas, development of process for the production of high BTU gas from coal becomes more attractive, and is now under extensive investigations, most of which are sponsored by the Office of Coal Research, Department of the Interior. The overall system for production of the pipeline gas consists of several unit processes such as gasification, water-gas shift conversion, gas purification and methanation. In the present study, the water-gas shift conversion process of a large commercial scale is optimized in connection with the primary gasification and methanation processes. The objective is to search the most economical scheme for shift conversion by which the effluent gas from the gasifier can be processed to achieve a proper hydrogen-to-carbon monoxide ratio for methanation at a later stage. Conditions and compositions of raw gas vary depending on the different primary gasification processes from which it emerges. Among the various gas compositions obtainable, two cases are selected as shown in Table 1. These selections will meet the following requirements imposed on methanation: (1) production rate of pipeline gas is 250×10^9 BTU/day; (2) heating value of pipeline gas is more than 900 BTU/SCF.

2. REACTION KINETICS

A. Rate Equations

The stoichiometric relation of water-gas shift reaction is expressed by

$$CO + H_2O = CO_2 + H_2 \qquad (1)$$

In addition to the above reaction, thermodynamically it is possible that several other side reactions may take place among the components of CO, H_2O, H_2, CO_2, CH_4 and other hydrocarbons. These reactions involve the methane formation and the carbon deposition. Presently however the well developed commercial iron-chromium-oxide catalyst is employed under the suitable steam to gas ratio which is obtained based on equilibrium considerations, showing a satisfactory selectivity in most water-gas shift conversion processes. In this study therefore only reaction (1) will be of primary importance.

Among the different types of water-gas shift rate equations proposed so far, the first order equation of Laupichler [11], Mars [13], the second order equation of Moe [15], and the exponential form of equation of Bohlbro and others [4] are noteworthy. The recent paper of Ruthven[18] reviewed the experimental results obtained by previous investigators, and concluded that the pseudo first order rate equation is quite adequate in most cases. This equation seems to have more flexibility than others since it includes the pore diffusion effect of catalyst, which is particularly important at high temperatures.

Table 1. Flow Rates and Compositions of Feed and Product Gases

Low CO Case

	Feed		Product (dry basis)	
	lb-mole/hr	mole %	lb-mole/hr	mole %
CO	9209.0	11.78	6446.3	10.43
H_2O	19155.8	24.50	--	--
H_2	17817.4	22.79	20580.1	33.31
CO_2	11567.3	14.79	14330.0	23.19
CH_4	19721.0	25.22	19721.0	31.91
N_2	716.3	0.92	716.3	1.16
Total	78186.8	100.00	61793.7	100.00

Inlet Temperature: 1000°F Pressure: 1100 psia

High CO Case

	Feed		Product (dry basis)	
	lb-mole/hr	mole %	lb-mole/hr	mole %
CO	31850.6	35.32	12421.7	12.69
H_2O	11767.5	13.04	--	--
H_2	19220.3	21.30	38649.2	39.49
CO_2	12002.9	13.30	31431.8	32.11
CH_4	14591.7	16.17	14591.7	14.91
N_2	784.5	0.87	784.5	0.80
Total	90217.5	100.00	97878.9	100.00

Inlet Temperature: 1700°F Pressure: 1050 psia

In the present study, the pseudo first order rate equation is consistently used regardless of operating conditions. However, the result obtained from the second order equation of Girdler[7] is also presented for comparison. The two types of rate equations are summarized as follows:

(a). Pseudo first order rate equation

$$-\frac{dp}{dt} = k_o\,(p-p_e) \tag{2}$$

or in an integrated form

$$-\ln\,(1-X/X_e) = k_o t = k_{a_p}/S_v \tag{3}$$

The value of K_{a_p} is obtained from intrinsic catalyst activity, k_s as follows:

$$k_s = 1079\,\exp(-27300/RT) \tag{4}$$

$$k_{v_1} = \rho_p S_p\, RT\, k_s \tag{5}$$

$$D_{e_1} = 0.069\,(T/673)^{3/2} \tag{6}$$

$$\Phi_1 = 0.5 d_p\,(k_{v_1}/D_{e_1})^{1/2} \tag{7}$$

$$\eta_1 = \frac{3}{\Phi_1}\left(\frac{1}{\tanh\Phi_1} - \frac{1}{\Phi_1}\right) \tag{8}$$

$$k_{a_1} = 492\, k_{v_1}\, \eta_1\, (1-\varepsilon)/T \tag{9}$$

$$k_{a_p} = k_{a_1}[(P/14.7)^{0.35} - 1/\Phi_1]/(1-1/\Phi_1) \tag{10}$$

(b). Second order rate equation

$$r'_{CO} = k(C_{CO}\,C_{H_2O} - C_{H_2}\,C_{CO_2}/K_y) \tag{11}$$

$$k = \exp(15.95 - 17500/RT) \tag{12}$$

B. Mass and Heat Transfer Within Catalyst Bed

Since the water-gas shift reaction is comparatively slow and moderately exothermic, the difference in temperature and concentration between bulk phase of gas and catalyst surface is not expected to be very great. This can be shown numerically as follows. The temperature difference may be estimated by:

$$T_c - T_b = r_s \Delta H/(h_p \pi d_p^2) \tag{13}$$

where h_p is the heat transfer coefficient between the particle surface and bulk phase, and can be calculated from [23]

$$J_H = (N_{Pr})^{2/3} h_p/(C_p G) = 0.989 (d_p G/\mu)^{-0.41} \quad (14)$$

The maximum temperature difference will result from the maximum reaction rate. The calculation based on the value, r_{CO} = 6 lb-mole CO/(hr. cu. ft. cat.), G = 7000 lb/(hr.sq. ft.) shows approximately $(T_c - T_b) \approx 3°F$. Such a negligibly small temperature difference was also reported earlier [11], [13]. The temperature gradient within a catalyst pellet can be calculated by the following heat balance equation, assuming an uniform reaction rate in the catalyst.

$$\frac{d^2T}{dr^2} + \frac{2}{r}\frac{dT}{dr} = \frac{r_{CO}}{k_e}\Delta H \quad (15)$$

where k_e, the effective thermal conductivity may be calculated from

$$\frac{1}{k_e} = \frac{1}{(1-\zeta)k_c + \zeta k_g} \quad (16)$$

Solution of the above equation using proper boundary condition is

$$T = T_c + \frac{1}{6}\left(-\frac{r_{CO}}{k_e}\Delta H\right)\left[\left(\frac{d_p}{2}\right)^2 - r^2\right] \quad (17)$$

Again r_{CO} = 6 lb-mole/ (hr.cu.ft.cat.) is used for the calculation of temperature difference within the pellet, yielding that $(T-T_c)|_{r=o} < 4°F$.

In a similar manner, the concentration difference between the bulk phase and the surface of the catalyst is approximated by

$$C_c - C_b = r_s/(k_f \pi d_p^2) \quad (18)$$

where k_f is the fluid-particle mass transfer coefficient in the bed, and may be evaluated from [9]

$$\frac{J_M}{(1-\varepsilon)^{0.2}} = 1.40\left[\frac{d_p G}{\mu(1-\varepsilon)}\right]^{-0.41} \quad (19)$$

The numerical calculation indicates that the maximum difference in concentration corresponds to only 2% of bulk phase concentration.

In summary, it may be safely assumed that the differences in temperature and concentration between the bulk phase and the catalyst surface are negligibly small.

3. PERFORMANCE EQUATIONS

A. Flow Model for Fixed Bed Reactor

Flow patterns of fluid in a fixed bed reactor are describable by the dispersed-plug flow model or compartment-in-series model. The required condition may be specified as follows [12]

$$D_a/vL < 0.01 \tag{20}$$

Noting the relation $D_a/vL = (D_a/vd)(d/L)$

and using the experimental results of Levenspiel and Bischoff [12],

$$D_a/vd \approx 0.5 \tag{21}$$

Equation (20) is equivalent to $d/L < 0.02$ (22)

In this study the characteristic length d is the same as the unit compartment length which is selected as 1 in. Therefore, it is seen from equation (22) that if L is larger than 5 ft. the requirement is satisfied.

B. Performance Equations for Reactor Simulation

Material balances for each component around n-th compartment are given as follows:

$$F_i^n = F_i^{n-1} + V_c^n r_{CO} \qquad i = 1,2,\cdot\cdot,6 \tag{23}$$

r_{CO} is negative for i=1,2, positive for i=3, 4, zero for i=5,6, where F_1^n, F_2^n, F_3^n, F_4^n, F_5^n, F_6^n are the molar flow rate of CO, H_2O, H_2, CO_2, CH_4, and N_2 at the exit of the n-th compartment, respectively; V_c^n is the catalyst volume per unit compartment. Energy balance around the n-th compartment under adiabatic conditions may also be expressed as:

$$-(T^{n-1}-T_o)\sum_{i=1}^{6} F_i^{n-1} C_{p_{im}} + (T^n - T_o)\sum_{i=1}^{6} F_i^n C_{p_{im}} = -\Delta H_{T_o} V_c^n r_{CO} \tag{24}$$

where $C_{pim} = \int_{T_o}^{T} C_{pi}\, dT/(T - T_o)$, $\Delta H_{T_o} = -17698$ BTU/lb-mole

The pressure effect on heat capacities may be considered negligible even at 1000 psig except for steam.

Pressure drop through the fixed bed reactor is calculated using Ergun's equation [8]:

$$\Delta P = \frac{150(1-\varepsilon)\,\mu/(d_p G) + 1.75}{\left(\frac{\varepsilon^3}{1-\varepsilon}\right)\left(\frac{d_p}{C_L}\right)\left(\frac{\rho g}{G^2}\right)} \tag{25}$$

C. Design Equation for Heat Exchanger

Considering the change of film coefficient and scaling problem, it is assumed that approximately 50% of water entering the tubes in heat

exchangers is evaporated to generate steam. Then the heat balance can be written as:

$$Q = W_s C_p (T_2 - T_1) \quad \text{for shell side} \tag{26}$$

$$= W_T [C'_p (t_2 - t_1) + 0.5\lambda] \quad \text{for tube side} \tag{27}$$

where T_1, t_2 are the outlet temperatures, and T_2, t_1, are the inlet temperatures of shell side and tube side, respectively. The shell side heat transfer coefficient is calculated from:

$$(h_o D_o / k_g) = 0.36 (D_o G_s / \mu)^{0.55} (C_p \mu / k_g)^{1/3} \tag{28}$$

The pressure drop in the shell side is estimated by the following equation [10]:

$$\Delta P = f_s G_s^2 D_s L_H / (5.22 \times 10^{10} D_{os} B) \tag{29}$$

where

$$f_s = 0.01185 (D_o G_s / \mu)^{-0.1876} \tag{30}$$

The tube side heat transfer coefficient for the case without phase change* may be computed by:

$$(h_i D_i / k_w) = 0.027 (D_i G_i / \mu_w)^{0.8} (C'_p \mu_w / k_w)^{1/3} (\mu_w / \mu_o)^{0.14} \tag{31}$$

Since a complete optimal design of heat exchangers is rather involved which is not called for in this study, a simplified procedure is adapted. This procedure involves the determination of an optimum heat transfer coefficient for the heat exchanger. Clearly the increasing mass velocity of gases will have a favorable effect on heat transfer coefficient but will result in a larger pressure drop. An optimum heat transfer coefficient therefore is calculated based on the highest velocity within the allowable pressure drop of 3 psi.

4. ECONOMIC INFORMATION

A. Equipment Cost

Reactor Shell Cost: The thickness of the reactor wall, T_h is computed from [1]

$$T_h = P R' / (S_r E' - 0.6P) \tag{32}$$

and weight of reactor W_R which includes the top and bottom blank is calculated by

$$W_R = \frac{\pi}{4} \rho_m \left[\left\{ (D + \frac{T_h}{6})^2 - D^2 \right\} L + \frac{F_d^2 T_h}{6} \right] \tag{33}$$

*See appendix for the case of phase change.

Then the reactor cost becomes $E_R = C_R I_f W_R$ (34)

Cost of catalyst supporting trays : $E_S = 0.216\ I_f N(D+5)^{3.13}$ (35)

Control Valve Cost: Average values of \$8000 per valve for a large single reactor and \$4000 for small parallel reactors are used.

Heat Exchanger Cost [17]: $E_H = C_y I_f\ [850\ (A_T/50)^{0.562}]$ (36)

Pump Cost: The following equations are used to estimate the cost of pumps [6] [14] associated with heat exchangers to deliver cooling water

$$E_p = 684\ B_p^{0.467} \tag{37}$$

where

$$B_p = q\ \rho_w\ \Delta h/(246{,}800\ E_f) \tag{38}$$

B. Cost of Direct Material and Utility

Catalyst Cost: $E_c = I_c V_c$ (39)

Steam Cost: Although the cost of steam depends largely upon its source and manufacturer, a value of 60 cents per thousand pounds is primarily used.

Thus $E_{ST} = (W_{ST}/1000)\ (8200)\ (0.6)$ (40)

Cooling Water Cost: \$0.12 per thousand gallon is used for treated water.

Electricity Cost: 11 mil per kw-hr is used

C. Calculation of Revenue Requirement

In order to optimize the process, formulation of objective function is necessary. The objective function is developed based on the annual cost. The accounting procedures is "Utility Gas Production General Accounting Procedure" which is formulated by the American Gas Association and adopted by the Office of Coal Research. The procedure estimates the annual revenue requirement under the following conditions [21]:

Debt-equity structure	65% debt (1/20th retired annually)
Return on-rate base	7%
Federal income tax rate	48%
Interest on debt	5%
Depreciation, 20 year straight line	5%
State and local taxes and insurance	3%

The revenue requirement is composed of three factors: operating costs, return-on-rate base; and federal income taxes. In current optimization raw material cost is not considered and one man per shift is assumed for operating labor. The steam cost is calculated separately from the revenue requirement, because of the difficulty as well as the importance of steam cost estimation in optimization.

5. OPTIMIZATION

A. Process Description

The block diagram of the system for optimization is shown in Figure 1. Since the temperature of the raw gas from gasifier is usually much higher than the operating temperature for shift conversion, cooling by waste heat boiler is necessary before going into the reactor. The gas after cooled to a proper temperature is then introduced to the reactor in which the mole ratio of carbon monoxide to hydrogen is adjusted about 1/3. Therefore, for any fixed inlet gas composition, there is always a required conversion of carbon monoxide. Before the gas enters the reactor, a certain amount of steam is added to this stream. The additional steam also brings the steam to gas ratio high enough so that carbon deposition on catalyst will not take place. Determination of the proper steam to gas ratio is not a simple problem, however, because it requires the knowledge of many factors including the reaction kinetics of carbon with gases. Furthermore, the amount of steam introduced would greatly affect not only the steam cost but also reaction rate, equilibrium conversion, etc. and the optimum operating conditions.

The required conversion of carbon monoxide can be achieved in the reactor by one throughput. However, because of the cost of steam and the heavy duty required in the product gas cooler, it will be more advantageous to by-pass a portion of the feed, and mix it with the product gas that has been converted in excess in the reactor. The conversion in the reactor is adjusted to achieve the required conversion upon mixing. It is observed that in order to meet the required conversion by this scheme, the conversion in the reactor has to approach closely to the equilibrium conversion. The temperature of product gas after the shift conversion is approximately 900°F, or lower if this product is mixed with the by-passed gas. Again, it is required to cool the outlet gas before purification. The outlet temperature of product gas cooler should be decided based on the performance of purifier, but in the present study this temperature is fixed at 460°F for convenience.

B. Adiabatic Reactor

The adiabatic operation can be represented on the conversion-temperature plot. Figure 2 shows the equilibrium curves for different values of steam to gas ratio based on the feed composition of the low CO case. On the same figure are shown the adiabatic operating lines

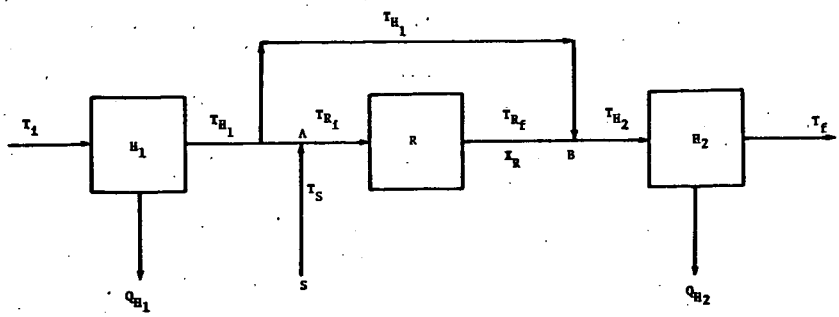

Figure 1 Block Diagram of Water-Gas Shift Conversion System Considered for Optimization

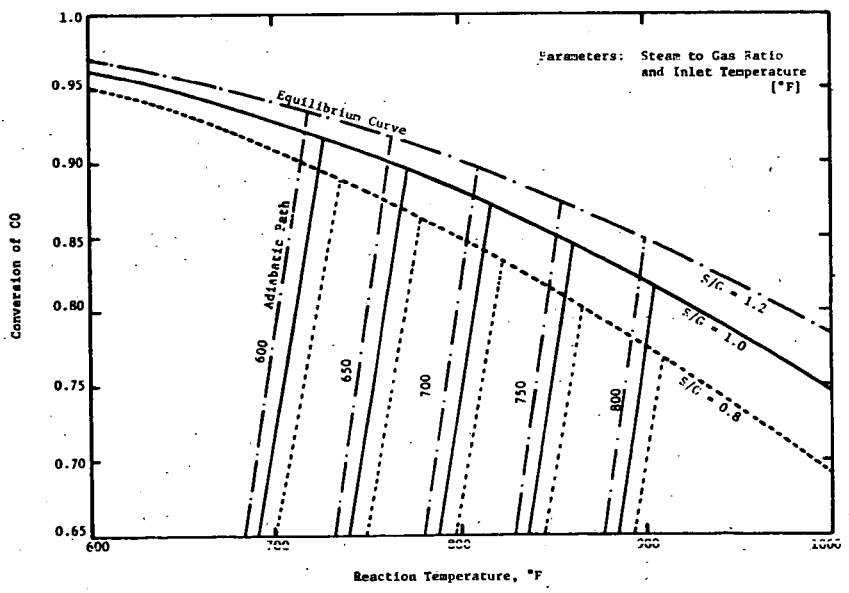

Figure 2 Reaction Paths in Adiabatic Reactor for Low CO Case

which represent the energy balance relationship starting from the given inlet temperatures. The intersection of adiabatic path with equilibrium curve is adiabatic-equilibrium point, indicating the maximum attainable conversion and temperature in an adiabatic operation. The inlet gas temperature to reactor is one of the decision variables, having an allowable range between 600°F to 800°F. The maximum allowable operating temperature is selected as 900°F, because experimentally it has been shown that undesirable phenomena such as catalyst sintering and carbon deposition could take place above this temperature.

The optimization of reactor part is to find the reaction conditions at which the total annual cost is minimized. However, since the entire system to be optimized includes heat exchangers also, the optimum conditions cannot be decided from the reactor study alone. In other words, the reactor is regarded as one stage while the entire process constitutes a multi-stage process. Therefore, at each stage the optimal decisions are obtained for every admissible value of state variables. In this study the quantities to be decided for the optimization of the reactor are: the inlet gas temperature, the conversion (or by-pass fraction), and the diameter of reactor. If we select the temperature of gas as the state variable and the remaining quantities as the decision variables, then the reactor optimization will follow the procedure of searching for the optimum conversion and optimum diameter for every admissible value of the inlet gas temperature.

It can be proven that for a given reactor volume, a smaller diameter reactor weighs less than that of a larger diameter reactor because of the thickness of the reactor wall. Therefore, once the volume of the reactor is determined from the conversion, the smallest diameter will be chosen as the optimum diameter which offers the allowable pressure drop through the reactor. This reduces the number of decision variables and simplifies the calculation.

The procedure of reactor optimization is as follows:

1. The adiabatic equilibrium conversion and temperature are determined for each of the assumed inlet temperatures with given feed composition.
2. An initial trial value of diameter is estimated approximately from the required conversion, the average temperature and the pressure of the gas stream.
3. Starting from the point near the equilibrium conversion, the annual cost for the reactor part is calculated at each point along the adiabatic line by a suitable interval of conversion. In this procedure, search methods such as Fibonacci Search or Golden Section Search may be used for higher efficiency, but in the present study a constant interval of 0.05 is taken for simplicity. Meanwhile, at each conversion the correct diameter of the reactor satisfying the pressure drop limitation is calculated by iterations. It is noted that the determination of conversion in the reactor fixes automatically the by-pass fraction of the feed gas.
4. Once the optimum conversion and the correct value of the diameter is obtained for a single reactor, the optimum number of reactors in

parallel can be decided readily, based on the optimum space velocity already determined.

After the heat exchanges and reactor are optimized individually for every admissible inlet and outlet gas temperatures, the results can be combined to locate the optimum temperatures for the overall system. To accomplish this, first it is necessary to decide the steam temperature, T_s, in Figure 1. Apparently, the increasing value of T_{H_1} favors the cost of H_1 but affects that of H_2 adversely if T_{R_f} is fixed. These two opposite tendencies can be combined to show that the highest possible T_{H_1} and consequently the lowest possible T_S should be selected for an economical operation. In this study T_S is selected as the saturation temperature of steam at the operating pressure. Once the temperature of steam is fixed, the remaining procedure is straightforward. For every value of T_{R_i} the value of T_{H_1} is calculated by material and energy balances around point A. Since the corresponding value of T_{R_f} is already obtained by an optimum X_R in the reactor, similar material and energy balances around point B yield the value of T_{H_2}. Hence, all the necessary inlet and outlet temperatures for estimating the overall costs are determined.

C. Cold-Quenching Reactor

The adiabatic system provides a simple and economical process when the concentration of carbon monoixde in the feed gas stream is low. However, when the CO concentration is high the rate of heat evolution is so high that the removal of heat from the system becomes necessary in order to keep the reaction temperature within the desirable range. Hence, from the point of temperature control, more flexible cold-quenching system must be employed. In water-gas shift converter cold-quenching is achieved by injecting a suitable amount of cold water and vaporizing it in the quenching zone of the reactor. Since steam is a reactant and is required in excess, the water-quenching accomplishes dual effects: temperature reduction and steam supply. Figure 3 (a) shows the present system of cold-quenching water-gas shift conversion process. In the first reaction zone the reaction progresses under an adiabatic condition. When the reaction has achieved a certain extent of conversion, the quenching is performed in the quenching zone by a pressurized low temperature cooling water which is completely vaporized and mixed with the reacting gas stream before entering the next reaction zone. Care must be exercized for the design and operation of quenching zone to assure complete vaporization of water in the quenching zone, otherwise the unvaporized water will drastically contaminate the catalyst in the subsequent reaction zone. After quenching, the low temperature gas continues to react in the second reaction zone. The alternate quenching and reaction continue until the desired conversion is achieved. The cooling process in the product gas cooler which follows the reactor is the same as that of the adiabatic system.

Since the cold-quenching system consists of a series of adiabatic beds, the typical optimization technique for multi-stage process, namely dynamic programming is used. In this study, a three-stage system is selected based on the results of simulation. The backward dynamic program is expressed by the well known Bellman's principle of optimzality [2] as: "Whatever the initial state and decisions are, the remaining decisions must constitute an optimal policy with regard to the state resulting from the first decision." In contrast to the backward dynamic program algorithm, a forward dynamic program algorithm [3] has been proposed as: "Whatever the ensuing state and decisions are, the preceding decisions must constitute an optimal policy with regard to the state existing before the last decision." The selection of backward or forward algorithm will depend on the type of problem as well as the given boundary conditions.

In Figure 3(a) the initial state (X^I, T^I), and final state (X^F,T^F) are fixed as described earlier, but all other values at intermediate stages must be determined by optimization. Now from the relationship between the value of X_3^f and the amount of gas by-passed, it is possible to confine the system of optimization to the region surrounded by the dotted line in Figure 3(a). Figure 3(b) shows the modified system to be optimized with X_1^i given.

Each stage except stage 1 consists of one quenching zone and one reaction zone, and has two state variables X, T, and two decision variables W and ΔX. For example, if we use backward algorithm in stage 3, for any given value of (X_3^i, T_3^i), we can find the optimal decision W_3 and ΔX_3 such that the total cost is minimized. In stage 1 although no quenching water W, is used, the principle of computational procedure is still the same.

Generally, a backward approach has been used more frequently, and can be also applied to the present problem. However, in this study the forward concept is used because firstly, the problem is of initial condition type, and secondly, the equilibrium constraint existing at the end of each stage is helpful for taking the admissible ranges of state variables.

The general recurrance formula in N-stage process is

$$F_N(\bar{Y}_N) = \underset{\{\bar{0}_N\}}{\text{Min}} \left[G_N(\bar{Y}_N, \bar{0}_N) + F_N(\bar{Y}_N)\right] \qquad (40)$$

where

$\bar{Y}_N$ and $\bar{0}_N$ are the state and decision vectors at the N-th stage

G_N and F_N are the objective and minimum objective function, respectively.

Then the following functional equation can be written for each stage.

First stage, $$F_1(X_1^f, T_1^f) = \underset{\{\Delta X_1\}}{\text{Min}} [G_1 (X_1^f, T_1^f, \Delta X_1)] \quad (41)$$

Second stage, $$F_2(X_2^f, T_2^f) = \underset{\{\Delta X_2, W_2\}}{\text{Min}} [G_2(X_2^f, T_2^f, \Delta X_2, W_2) + F_1(X_1^f, T_1^f)] \quad (42)$$

Third stage, $$F_3(X_3^f, T_3^f) = \underset{\{\Delta X_3, W_3\}}{\text{Min}} [G_3(X_3^f, T_3^f, \Delta X_3, W_3) + F_2(X_2^f, T_2^f)] \quad (43)$$

Based on the above equations and using the material and energy balance relations, the optimization is performed starting from the first stage. Although the system is different and involves the multi-dimensionality problem, the basic principle for optimization at each stage is quite similar to that of the adiabatic system. In each case the amount of quenching water is adjusted within the capacity of quenching zone, and the intervals of variables are properly selected based on the sensitivity of objective function and on the computing time. A linear interpolation approximation is applied to connect the stages. The computational procedure is as follows:

1. At the exit of the first stage, the admissible ranges of X_1^f and T_1^f are found. In doing this, the restricted range of operating temperature, $550°F \leq T \leq 900°F$, and the equilibrium temperature-conversion relationship are considered. Then within the range the netwise two-dimensional lattice points of (X_1^f, T_1^f) are formulated.

2. The corresponding T_1^i for each of the lattice point is calculated using material and energy balance relationship in the stage. The size of reactor is evaluated, the annual cost, G_1, is then obtained and tabulated.

3. Similarly, at the exit of the second stage the admissible values of (X_2^f, T_2^f) are found.

4. (X_2^i, T_2^i) 's are calculated for different values of $(\Delta X_2, W_2)$, and the evaluated G_2's are listed.

5. Interpolation is performed between (X_1^f, T_1^f) and (X_2^i, T_2^i), and the minimum values of (G_1+G_2) obtained are listed for every value of (X_2^f, T_2^f).

6. By a similar computation at the third stage, all the values of (X_3^i, T_3^i) and G_3 are also obtained from the admissible values of (X_3^f, T_3^f) and $(\Delta X_3, W_3)$.

7. Interpolation is performed between (X_2^f, T_2^f) and (X_3^i, T_3^i). Hence, the total objective function $(G_1+G_2+G_3)$ is obtained for every value of (X_3^f, T_3^f), from which the optimum result is found.

Again the reactor part and heat exchanger part can be combined by the similar procedure shown in adiabatic system.

6. RESULTS

Adiabatic system: Figure 4 shows the reaction rate profiles along the reactor and Figure 5 illustrates the annual cost .vs. reactor inlet temperature for the low CO case. The optimum operating conditions and corresponding costs are listed in Tables 2 and 3 for both the low CO case and the high CO case.

Cold-quenching system: The reaction rate profile for the low CO case, and reaction paths for both cases are shown in Figures 6 to 8, respectively; the optimum operating conditions and costs are listed in Tables 4 to 6.

7. DISCUSSION

A. Effect of Steam to Gas Ratio on Optimization of Adiabatic Water-Gas Shift Conversion System

As already indicated, the steam to gas ratio is one of the most important factors in the optimization of water-gas shift conversion system. However, its determination is not straightforward. To see how this factor affects the performance of the reaction and the optimization, different values of steam to gas ratio were employed for the low CO case in the adiabatic system. Figure 9 shows the reaction rate profiles along the reactor height with different steam to gas ratios of 0.8, 1.0, and 1.2. The operating conditions and costs are listed in Table 7, indicating that the major difference in cost comes from the variation in the amount of steam although there is also a considerable change in other costs.

B. Effect of Pressure on the Reactor Performance

Since little is known about the reaction kinetics above 450 psig, the validity of rate equation used in this study is uncertain above this pressure. Besides, most of the commercial plants are operated around 400 psig or less, due to the experimental fact that the activity of iron-chromium-oxide catalyst increases rapidly with pressure in the low pressure range but above 400 psig, the effect of pressure becomes insignificant.

Two additional operating pressures of 300 psig and 600 psig are selected to study the effect of pressure on the adiabatic reactor operation. Figure 10 shows the profiles of reaction rate and Table 8 lists the operating conditions and costs. These results indicate that at high pressure although the reaction rate is increased and consequently the volume of reactor is decreased, the cost of reactor becomes higher because of the reactor wall thickness. Therefore, in general, there is no reason to operate the reaction at a high pressure unless other parts of the gasification processes are conducted under high pressures.

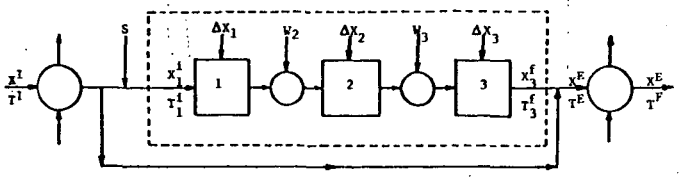

Figure 3(a)

X: Conversion of CO
T: Temperature
S: Steam
W: Quenching Water

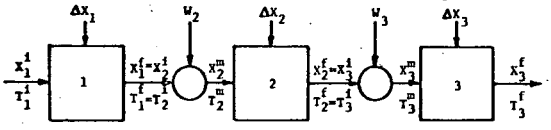

Figure 3(b)

Figure 3 Block Diagram of Cold-Quenching Water-Gas Shift Conversion System Considered for Optimization

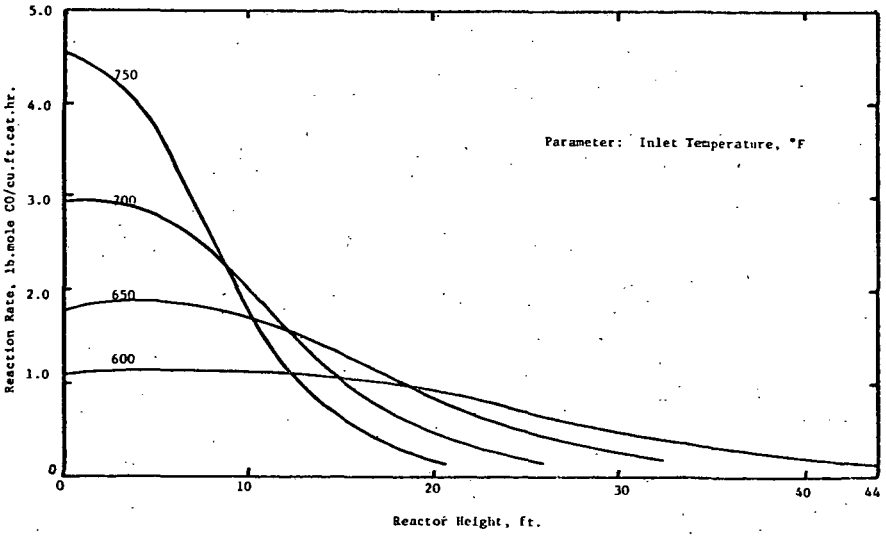

Figure 4 Reaction Rate Profiles in Adiabatic Reactor for Low CO Case

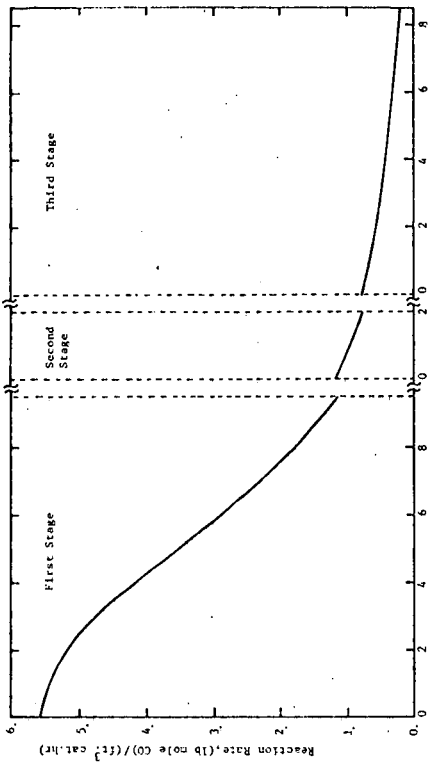

Figure 6 Reaction Rate Profile Under Optimum Condition in Cold-Quenching Reactor for Low CO Case

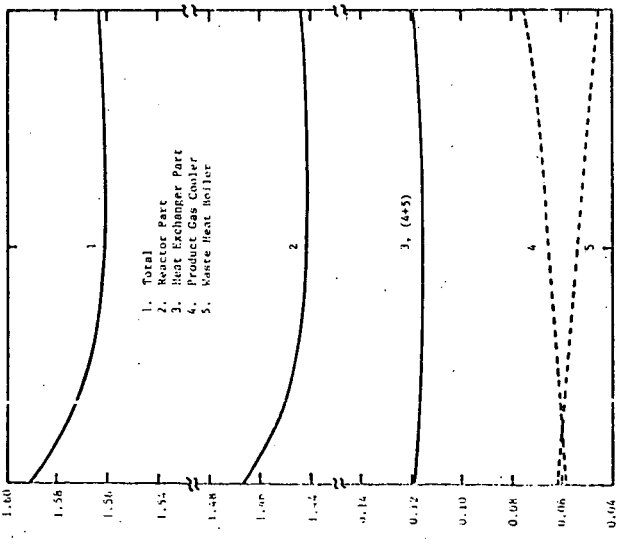

Figure 5 Total Annual Cost in Terms of Reactor Inlet Temperature Indication 700°F is Optimum for Low CO Case

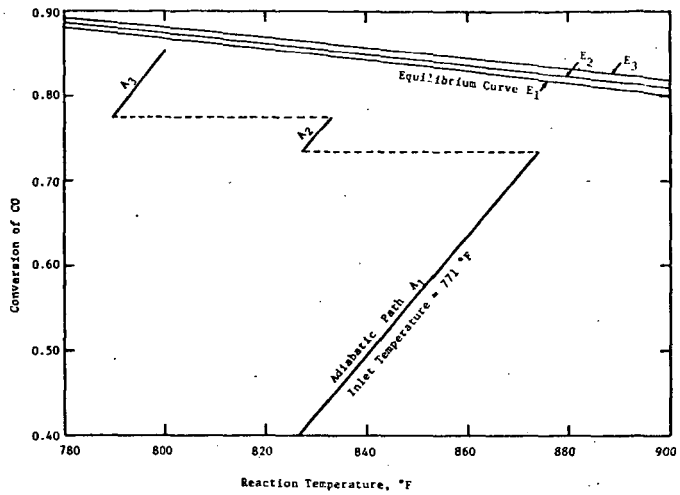

Figure 7 Reaction Path Under Optimum Condition in Cold-Quenching Reactor for Low CO Case

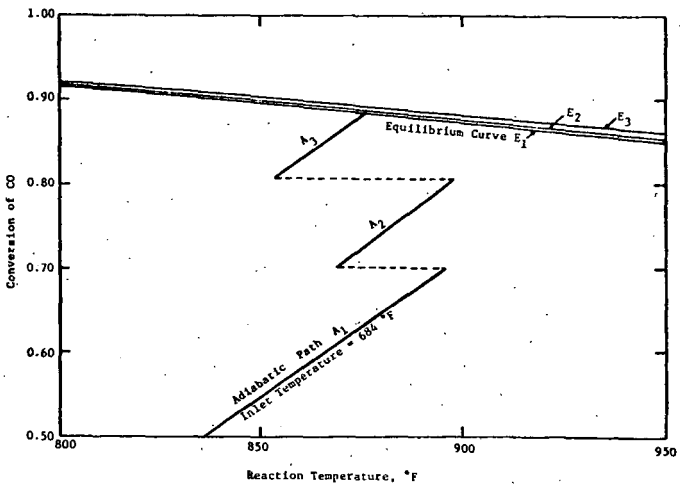

Figure 8 Reaction Path Under Optimum Condition in Cold-Quenching Reactor for High CO Case

Table 2. Optimum Operating Conditions In Adiabatic System

1. Reactor

	Low CO Case*	High CO Case†
Inlet Temperature, °F	700	650
Outlet Temperature, °F	815	899
Conversion of CO	0.855	0.883
Fraction of Gas By-passed	0.649	0.309
Space Velocity, hr^{-1} (dry gas at 60°F, 1 atm)	4380	3890
Temperature of Steam Supplied, °F	556	551
Number of Parallel Reactors	3	11
Diameter, ft.	7.0	6.7
Height, ft.	25.9	22.7
Thickness, in	3.7	3.4
Catalyst Amount/unit, cu. ft.	600	480

Steam to gas ratio selected: *1.0, †1.6

2. Heat Exchangers

Low CO Case	Waste heat Boiler	Product Gas Cooler 1	Product Gas Cooler 2
Inlet Temperature of Gas, °F	1000	788	704
Outlet Temperature of Gas, °F	765	704	460
Number of Heat Exchangers	6	5	6
Flow Rate of Gas/unit, M lb/hr	247.4	347.4	289.5
Flow Rate of Water/unit, M lb/hr	58.5	30.6	78.4
Temperature of Steam Produced, °F	556	556	250
Heat Load/unit, MM BTU/hr	32.3	16.9	40.3
Heat Transfer Area/unit, sq. ft.	850	733	1162
Heat Transfer Coefficient, BTU/(hr.sq.ft.°F)	88.1	79.3	92.5

Table 2. (Continued)

High CO Case	Waste Heat Boiler	Product Gas Cooler 1	Product Gas Cooler 2
Inlet Temperature of Gas, °F	1700	878	570
Outlet Temperature of Gas, °F	771	570	460
Number of Heat Exchangers	10	17	10
Flow Rate of Gas/unit, M lb/hr	192.7	196.1	333.5
Flow Rate of Water/unit, M lb/hr	151.9	62.2	36.8
Temperature of Steam Produced, °F	551	551	250
Heat Load/unit, MM BTU/hr	84.1	34.4	20.9
Heat Transfer Area/unit, sq.ft.	1262	1884	739
Heat Transfer Coefficient, BTU/(hr.sq.ft.°F)	91.4	66.9	90.6

Table 3. Equipment and Operational Costs In Adiabatic System

Low CO Case	Waste Heat Boiler	Reactor	Product Gas Cooler 1	Product Gas Cooler 2	Total
Reactor cost, M$	--	496.8	--	--	496.8
Catalyst cost, M$	--	36.3	--	--	36.3
Tray cost, M$	--	33.8	--	--	33.8
Control valve cost, M$	--	20.0	--	--	20.0
Heat exchanger cost, M$	41.2	--	34.2	49.1	124.5
Pump cost, M$	24.8	--	15.2	5.1	45.1
Cooling water cost, M$/yr	20.7	--	9.0	25.4	55.1
Working capital, M$/yr	4.7	20.7	2.4	3.3	31.1
Operating cost, M$/yr	49.2	167.8	24.4	33.9	275.3
Return on rate, M$/yr	2.8	22.6	2.0	2.3	29.7
Federal income tax, M$/yr	1.4	11.4	1.0	1.2	15.0
Revenue requirement, M$/yr	53.4	201.8	27.4	37.4	320.0
Steam cost, M$/yr	--	1240.2	--	--	1240.2
Total annual cost, M$/yr	53.4	1442.0	27.4	37.4	1560.2

Table 3. (Continued)

High CO Case	Waste Heat Boiler	Reactor	Product Gas Cooler 1	Product Gas Cooler 2	Total
Reactor cost, M$	--	1415.8	--	--	1415.8
Catalyst cost, M$	--	106.1	--	--	106.1
Tray cost, M$	--	94.8	--	--	94.8
Control valve cost, M$	--	52.0	--	--	52.0
Heat exchanger cost, M$	68.5	--	115.6	50.7	234.8
Pump cost, M$	63.0	--	70.7	6.2	139.9
Cooling water cost, M$/yr	89.6	--	62.5	21.8	173.9
Working capital, M$/yr	17.2	51.2	13.7	3.0	85.1
Operating cost, M$/yr	186.8	387.0	144.1	30.6	748.5
Return on rate, M$/yr	6.2	64.0	8.0	2.4	80.6
Federal income tax, M$/yr	3.3	32.1	4.1	1.2	40.7
Revenue requirement M$/yr	196.3	483.1	156.2	34.2	869.8
Steam cost, M$/yr	--	6965.5	--	--	6965.5
Total annual cost, M$/yr	196.3	7448.6	156.2	34.2	7835.3

Table 4. Optimum Operating Conditions In Cold-Quenching System for Low CO Case*

1. Reactor

	1st Stage	2nd Stage	3rd Stage
Inlet temperature, °F	771	827	812
Outlet temperature, °F	872	833	825
Conversion of CO achieved	0.735	0.775	0.855
Height of catalyst bed, ft.	9.5	2.0	9.0
Amount of quenching water, lb/hr	--	18,000	18,000
Temperature of quenching water, °F			500
Volume fraction of gas by-passed			0.649
Space velocity, hr^{-1} (dry gas at 60°F, 1 atm)			5490
Temperature of steam supplied, °F			556
Number of parallel reactors			4
Diameter, ft.			6.1
Height, ft.			26.5
Thickness, in.			3.3
Amount of catalyst/unit, cu. ft.			358
Amount of packing/unit, cu.ft.			58

*Steam to gas ratio selected: 0.9

Table 4 (Continued)

2. Heat Exchangers

	Waste Heat Boiler	Product Gas Cooler 1	Product Gas Cooler 2
Inlet temperature of gas, °F	1000	856	710
Outlet temperature of gas, °F	881	710	460
Number of heat exchangers	4	6	7
Flow rate of gas/unit, M lb/hr	371.1	290.7	249.2
Flow rate of water/unit, M lb/hr	44.9	42.7	68.8
Temperature of steam produced, °F	556	556	250
Heat load/unit, MM BTU/hr	24.8	23.5	39.0
Heat transfer area/unit, sq. ft.	517	873	1188
Heat transfer coefficient, BTU/(hr.sq.ft.°F)	98	82	87

Table 5. Optimum Operating Conditions in Cold-Quenching System for High CO Case*

1. Reactor

	1st Stage	2nd Stage	3rd Stage
Inlet temperature, °F	684	869	853
Outlet temperature, °F	895	898	876
Conversion of CO achieved	0.701	0.803	0.883
Height of catalyst bed, ft.	8.9	2.7	8.0
Amount of quenching water, lb/hr	--	32,400	57,600
Temperature of quenching water, °F			500
Volume fraction of gas by-passed			0.309
Space velocity, hr^{-1} (dry gas at 60°F, 1 atm)			4480
Temperature of steam supplied, °F			551
Number of parallel reactors			13
Diameter, ft			6.2
Height, ft			28.6
Thickness, in.			3.2
Amount of catalyst/unit, cu.ft.			353
Amount of packing/unit, cu. ft.			91

*Steam to gas ratio selected : 1.4

Table 5 (Continued)

2. Heat Exchangers

	Waste Heat Boiler	Product Gas Cooler 1	Product Gas Cooler 2
Inlet temperature of gas, °F	1700	867	570
Outlet temperature of gas, °F	823	570	460
Number of heat exchangers	9	15	9
Flow rate of gas/unit, M lb/hr	214.1	217.9	363.1
Flow rate of water/unit, M lb/hr	159.3	59.8	39.9
Temperature of steam produced, °F	551	551	250
Heat load/unit, MM BTU/hr	88.3	33.1	22.6
Heat transfer area/unit, sq. ft.	1218	1809	773
Heat transfer coefficient, BTU/(hr.sq.ft.°F)	104	68	94

Table 6. Equipment and Operational Costs in Cold-Quenching System

Low CO Case	Waste Heat Boiler	Reactor	Product Gas Cooler 1	Product Gas Cooler 2	Total
Reactor cost, M$	--	497.9	--	--	497.9
Catalyst cost, M$	--	28.6	--	--	28.6
Tray cost, M$	--	19.4	--	--	19.4
Control valve cost, M$	--	24.0	--	--	24.0
Heat exchanger cost, M$	24.8	--	41.8	54.2	120.8
Pump cost, M$	14.6	2.9	21.4	5.8	44.7
Cooling water cost, M$/yr	10.6	7.1	15.1	28.4	61.2
Working capital, M$/yr	2.5	29.2	3.7	3.6	39.0
Operating cost, M$/yr	26.0	270.0	38.0	37.8	371.8
Return on rate, M$/yr	1.7	22.6	2.6	2.5	29.4
Federal income tax, M$/yr	0.8	11.5	1.3	1.3	14.9
Revenue requirement, M$/yr	28.5	304.1	41.9	41.6	416.1
Steam cost, M$/yr	--	1056.6	--	--	1056.6
Total annual cost, M$/yr	28.5	1360.7	41.9	41.6	1472.7

Table 6 (Continued)

High CO Case	Waste Heat Boiler	Reactor	Product Gas Cooler 1	Product Gas Cooler 2	Total
Reactor cost, M$	--	1693.5	--	--	1693.5
Catalyst cost, M$	--	91.6	--	--	91.6
Tray cost, M$	--	64.5	--	--	64.5
Control valve cost, M$	--	60.0	--	--	60.0
Heat exchanger cost, M$	63.3	--	105.3	49.0	217.6
Pump cost, M$	58.0	4.2	61.2	5.8	129.2
Cooling water cost, M$/yr	84.6	17.7	52.9	21.2	176.4
Working capital, M$/yr	16.2	64.6	11.8	2.9	95.5
Operating cost, M$/yr	176.0	533.5	123.2	29.6	862.3
Return on rate, M$/yr	5.7	73.1	7.1	2.3	88.2
Federal income tax, M$/yr	3.1	36.8	3.7	1.2	44.8
Revenue requirement, M$/yr	184.8	643.4	134.0	33.1	995.3
Steam cost, M$/yr	--	6004.8	--	--	6004.8
Total annual cost, M$/yr	184.8	6648.2	134.0	33.1	7000.1

Table 7. Effect of Steam to Gas Ratio for Low CO Case

	S/G = 0.8	1.0	1.2
Inlet temperature, °F	700	700	700
Conversion of CO	0.815	0.855	0.877
Space velocity*, hr^{-1}	4290	4380	4640
Number of reactors	3	3	3
Diameter of reactor, ft.	6.7	7.0	7.3
Height of reactor, ft.	24.2	25.9	26.3
Thickness of reactor, in.	3.6	3.7	3.9
Reactor cost, M$	429.4	496.8	544.5
Catalyst cost, M$	31.1	36.3	39.7
Tray cost, M$	30.3	33.8	35.1
Control valve cost, M$	20.0	20.0	20.0
Bare cost, M$	479.7	550.6	599.6
Revenue requirement, M$/yr	182.4	201.7	215.3
Steam cost, M$/yr	915.8	1240.2	1567.0
Total annual cost, M$/yr	1098.2	1441.9	1782.3

*Based on dry gas at 60°F, 1 atm.

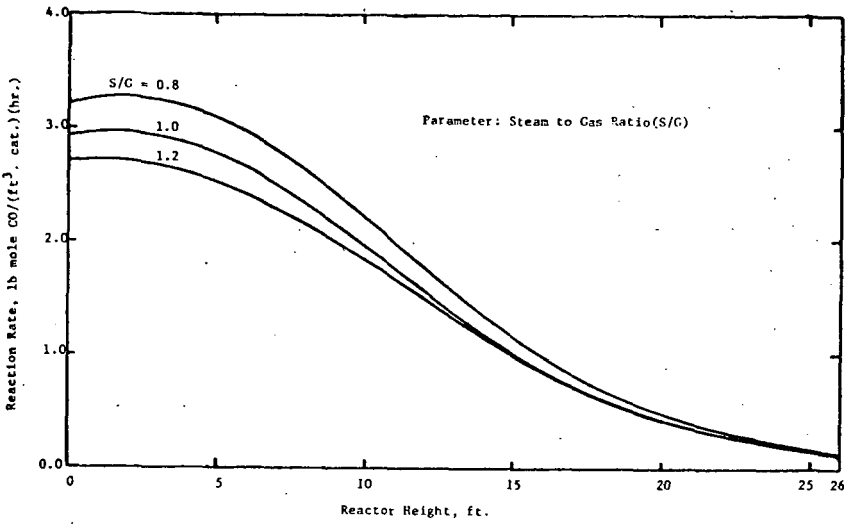

Figure 9 Effect of Steam to Gas Ratio on Reaction Rate in Adiabatic Reactor for Low CO Case

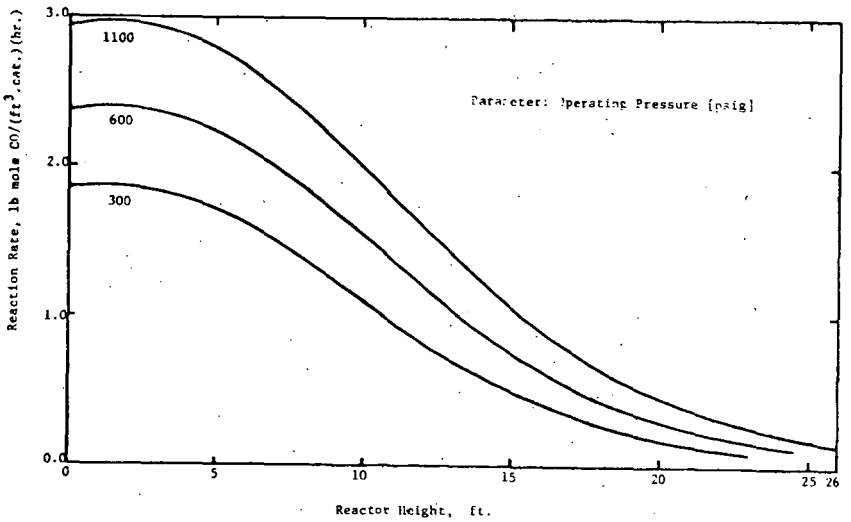

Figure 10 Effect of Operating Pressure on Reaction Rate in Adiabatic Reactor for Low CO Case

C. Comparison of the Results Using Different Reaction Rate Expressions

In section 2, two types of rate equation, namely the pseudo-first order equation (2) and the second order equation (11) are discussed. Since the design of the reactor depends greatly upon the rate equation, it will be necessary to compare the results obtained using the two rate equations. The operating conditions and the corresponding costs based on the two equations are listed in Table 9 for the adiabatic reactor. Because the applicable range of both equations favors low pressures, 300 psig is selected as the operating pressure. As can be seen from the table only small differences exist between the two results indicating that the water-gas shift reaction can be represented by either of the two equations in this range. The second order equation however seems to provide more conservative estimate than the first order equation.

D. Pressure Drop in Quenching Zone

Since the quenching zone is usually packed with rings and saddles, more pressure drop is expected in this region. Either of the following equations may be used for the approximation of pressure drop:

$$\Delta P/Z = 0.012\ C_f G^2/6g_c\rho \qquad (44)\ [20$$

or

$$\Delta P/Z = k' v^n \qquad (45)\ [1$$

If the values, G = 7000 lb/(ft^2 hr.) and ρ = 1.5 lb/ft^3 are used, then $\Delta P/Z$ = 0.05 psi/ft by equation (44) and 0.03 psi/ft by equation (45). Therefore the pressure drop through quencing zone in this study ca be neglected, unless the packing height is much larger than anticipated.

E. Effect of Sulfur Content in Gas

The sulfur content in gas is another important factor affecting greatly the performance of water-gas shift reaction. Therefore, if the amount of sulfur exceeds the allowable value, the catalyst activity deteriorates considerably requiring periodical generation. However, since the allowable sulfur content varies considerably depending on the type of catalyst used, the determination must be based on the experimental data obtained from the specific catalyst.

The study of Bohlbro [5] indicates that the kinetics of water-gas shift reaction may be modified by the presence of H_2S in the feed gas. According to his experimental results, if the content of H_2S is less than 100 ppm (part per million) only physical adsorption on the surface of catalyst takes place, but above 1000 ppm kinetics will be altered because

of the transformation of iron oxide into iron sulfide. On the other hand, Girdler [7] described that sulfur content above 150 ppm reduces the activity of catalyst greatly, but below 50 ppm sulfur does not have any significant effect on the activity of their catalyst. Mars [13] also discussed the effect of sulfur content on activity of catalyst showing removal of sulfur compounds from the feed gas increases the performance of reactor considerably.

The sulfur content in raw gas from the gasifier varies widely depending on the process, some of which could have as much as 0.9% of H_2S. However, this study is made based on the assumption that the sulfur content is small enough to be tolerated by the catalyst without causing substantial deactivation. In general, unless the sulfur content in the feed gas is very high, it is possible in most cases to select a proper type of catalyst that will withstand the sulfur poisoning for substantial length of time. On the other hand, if the catalyst gets deactivated it is also possible to modify the space velocity in the reactor to the corresponding reduction in catalyst activity. The recent study of Ting and Wan [19], shows another approach for handling sulfur-containing gases. Here the rate constant is modified by a sulfur correction factor, the value of which are obtained in terms of operating pressure up to 30 atm. for the gases containing H_2S as high as 0.24%.

F. Sensitivity Analysis

The current optimization involves a number of specific system parameters. But the information on these parameters are not necessarily accurate. Such an uncertainty of parameters is incurred by various internal and external factors and may affect the performance of optimization considerably under certain conditions. The sensitivity study here is intended to bring about a better system performance by analyzing the effect of variation in parameters on objective function. The sensitivity of a given parameter, S_e may be represented as [22]

$$S_e = [(J - \bar{J})/\bar{J}]/[(w - \bar{w})/\bar{w}] \qquad (46)$$

Referring to the results listed in Table 10, it is seen that the objective function is most sensitive to the parameters involved in kinetic expression. As is also expected, the dimension and character of catalyst pellet play an important role in the reactor performance.

Table 8 Effect of Pressure on Reactor Operation for Low CO Case

	300 psig	600 psig	1100 psig
Inlet temperature, °F	700	700	700
Conversion of CO	0.855	0.855	0.855
Space velocity*, hr^{-1}	2730	3540	4380
Number of reactors	3	3	3
Diameter of reactor, ft.	9.4	8.0	7.0
Height of reactor, ft.	23.0	24.5	25.9
Thickness of reactor, in.	1.5	2.4	3.7
Reactor cost, M$	259.8	358.0	496.8
Catalyst cost, M$	57.4	44.8	36.3
Tray cost, M$	49.2	42.0	33.8
Control valve cost, M$	20.0	20.0	20.0
Bare cost, M$	329.0	420.0	550.6
Revenue requirement, M$/yr	177.8	183.8	201.7
Steam cost, M$/yr	1240.2	1240.2	1240.2
Total annual cost, M$/yr	1418.0	1424.0	1441.9

Table 9 Comparison of the Results from First- and Second-Order Rate Equation at 300 psig for Low CO Case

	Eq. (2)	Eq. (11)
Inlet temperature, °F	700	700
Outlet temperature, °F	815.5	814.7
Conversion of CO	0.855	0.849
Space velocity*, hr^{-1}	2730	2030
Number of reactors	3	3
Diameter of reactor, ft.	9.4	9.9
Height of reactor, ft.	23.0	28.1
Thickness of reactor, in.	1.5	1.6
Reactor cost, M$	259.8	338.5
Catalyst cost, M$	57.4	70.3
Tray cost, M$	49.2	73.6
Control valve cost, M$	20.0	20.0
Bare cost, M$	329.0	432.1
Revenue requirement, M$/yr	177.8	219.4
Steam cost, M$/yr	1240.2	1248.9
Total annual cost, M$/yr	1418.0	1468.3

* Based on dry gas at 60°F, 1 atm.

Table 10 Parameter Sensitivity on Objective Function of Adiabatic Water-Gas Shift Conversion

Parameters	Sensitivity	
	Low CO Case	High CO Case
U_h	-0.3522×10^{-2}	-0.1218×10^{-2}
U_v	-0.8555×10^{-2}	-0.1977×10^{-2}
k_o	-0.3540×10^{-1}	-0.1902×10^{-1}
E	0.1452×10^{1}	0.7046×10^{0}
d_p	0.7971×10^{-1}	0.4530×10^{-1}
S_p	-0.3340×10^{-1}	-0.1847×10^{-1}
ρ_p	-0.3457×10^{-1}	-0.1892×10^{-1}
D_{e_p}	-0.3311×10^{-1}	-0.1832×10^{-1}
ϕ	-0.1181×10^{-2}	-0.1305×10^{-4}
Ψ	-0.7195×10^{-3}	-0.8584×10^{-5}

8. CONCLUSION

A. In the operation of water-gas shift reactor, steam cost occupies the major portion of the total cost. The reduction of the amount of steam is therefore most important in making the process more economical.

B. The total annual cost is not greatly affected by the variation in the reactor inlet temperature between 650°F to 750°F when the concentration of CO in the feed gas is low or moderate. For the gas of high CO concentration, however, the sensitivity due to the inlet temperature variation is increased.

C. The optimum conversion is very close to the equilibrium conversion in most cases, which is mainly due to the role of steam cost in the objective function.

D. Although the kinetics information of water-gas shift rection may not be accurate for high pressures, the operation beyond 400 psig does not seem to have any particular advantage.

E. In cold quenching reactor, major part of the total conversion is achieved in the first stage but both the first and the last stage of the reactor occupy the largest portion of overall reactor system.

F. The concentration of CH_4 and CO in the feed gas is the primary factor affecting the process cost. Because of the steam cost, the cold-quenching system is less costly than the adiabatic system in most cases, particularly in the high CO concentration case. However, if the steam can be ignored, the adiabatic system will be suitable for low CO concentration of less than 25% on dry basis.

G. From the sensitivity study, the objective function appeared to be somewhat sensitive to the parameters related to the kinetic expression and the character of catalyst pellet, indicating that special care must be exercised for the determination of these parameters.

ACKNOWLEDGMENT

The authors gratefully acknowledge the support of the Office of Coal Research, Department of the Interior, Washington, D.C.

NOMENCLATURE

A_1, A_2, A_3	Adiabatic paths in reaction zones of the first, second and third stages, respectively
A_h, A_v, A_T	Heat transfer areas of the heating zone, the vaporizing zone, and the total, respectively [sq.ft.]
B, B_p	Baffle spacing [ft.], and Brake horse power [hp.], respectively
C_i, C_b, C_c	Concentration of component i [mole frac.], and concentrations of product gas in bulk of gas phase and at catalyst surface [lb mole/cu.ft.], respectively
C_f	A constant related to the packings and fluid flow
C_L	Height of a unit compartment [ft.]
C_p, C'_p	Heat capacities of gases and water, respectively [BTU/(lb.°F)]
$C_{P_{im}}$	Molar temperature-mean heat capacity of component i [BTU/(lb mole,°F)]
C_R, C_y	Cost per pound of material used for construction of reactor shell [$/lb], and cost year index, respectively
d,D	Characteristic length in reactor and inside diameter of reactor, respectively [ft.]
D_a	Axial dispersion coefficient [sq.ft./hr.]
D_{e_1}, D_{e_p}	Effective diffusivity of CO in catalyst pores at 1 atm and at pressure p, respectively [sq.ft./hr.]
D_i, D_o, D_s	Inside diameter of tube, equivalent diameter for heat transfer tube, and inside shell diameter of heat exchanger, respectively [ft.]
d_p	Diameter of catalyst pellet [ft.]
E	Activation energy in pseudo first order rate equation [BTU/lb mole]
E', E_f	Efficiency of the longitudinal joints in cylindrical shells, and mechanical efficiency, respectively
E_c, E_{ST}	Cost of catalyst [$] and steam [$/yr], respectively
E_H, E_p, E_R, E_S	Costs of heat exchanger, pump, reactor and catalyst supporting tray, respectively [$]
Fd	flat blank diameter of top and bottom of domes of reactor [ft.]
F_i^{n-1}, F_i^n	Molar flow rates of component i at (n-1)-th compartment and n-th compartment, respectively [lb mole/hr]
f_s	Shell side friction factor [sq.ft./sq.in.]
g, g_c	Gravitational acceleration [ft./sq.hr.]
G	Superficial gas mass velocity [lb./(sq.ft.hr.)]
G_t, G_s	Mass velocity in tube side and shell side, respectively [lb/(sq.ft.hr.)]
Δh	Hydraulic head [ft.]
$\Delta H, \Delta H_{T_o}$	Heat of reaction at any temperature and at temperature T_o, respectively [BTU/lb mole CO]
h_i, h_o	Film heat transfer coefficient in inside and outside, respectively [BTU/(sq.ft.hr.°F)]
h_p	Fluid-particle heat transfer coefficient [BTU/(sq.ft.hr.°F)]
I_c, I_f	Unit cost of catalyst [$/cu.ft.] and cost factor, respectively
J,J	Objective function for a given value of parameter and that at the optimum condition, respectively
J_H, J_M	Heat transfer factor and mass transfer factor, respectively

K_y	Equilibrium constant based on mole fraction
k', n	Constants related to the packings and fluid flow
k	Reacton rate constant in second order rate equation [hr^{-1}]
k_{a_1}, k_{a_p}	Apparent catalyst activities at 1 atm and at pressure p, respectively [hr^{-1}]
k_c, k_e	Thermal conductivity of catalyst and effective thermal conductivity of catalyst particle, respectively [BTU/(ft.hr.°F)]
k_f	Fluid-particle mass transfer coefficient [ft/hr.]
k_g, k_w	Thermal conductivity of gas and water, respectively [BTU/(ft.hr.°F)]
k_o	Apparent first order rate constant based on the unit catalyst bed volume [hr^{-1}]
k_s	Intrinsic catalyst activity based on unit surface area [ft. lb mole/(hr.BTU)]
k_{v_1}	Intrinsic rate constant at 1 atm [hr^{-1}]
L, L_H	Lengths of reactor and heat exchanger, respectively [ft.]
N, N_{Pr}	Number of trays and Prandtl number, respectively
P, ΔP	Pressure of the system and pressure drop, respectively [lb_f/sq.in.]
p, p_e	Partial pressure of CO at any time and at equilibrium, respectively [lb_f/sq.in.]
Q	Heat transfer rate in heat exchangers [BTU/hr.]
q	Volumeric flow rate of water [gal./min.]
r	Radial distance in catalyst particle [ft.]
R	Gas constant [BTU/(lb mole, °R)]
R'	Inside radius of cylinder [in.]
r_{CO}, r'_{CO}	Reaction rate of CO [lb mole CO/(hr.cu.ft.cat.)], [cu.ft. CO/(hr.cu.ft.cat.)], respectively
R_d	Dirt factor in heat exchanger
r_s	Reaction rate per unit catalyst particle [lb mole CO/hr.unit cat.)]
s, S, S_e	Specific gravity, steam flow rate [lb/hr.] and sensitivity, respectively
S_p, S_r, S_v	Specific surface area of catalyst [sq.ft./lb], maximum allowable stress value [lb_f/sq.in.] and space velocity at N.T.P. basis [hr^{-1}], respectively
t	time [hr.]
T	Temperature, The subscript denotes the stage number and the superscript represents the status [°F] [°R]
T_1, T_2	Temperature of shell side at outlet and inlet, respectively [°F]
T_b, T_c	Bulk gas temperature in reactor and surface temperature of catalyst particle, respectively [°F]
T_h	Thickness of reactor shell [in.]
T_m	Shell side gas temperature at which vaporization of water starts to take place [°F]
T^{n-1}, T^n	Exit temperature of (n-1)-th compartment and n-th compartment, respectively [°F]
T_o, T_s	Standard temperature (77°F), and temperature of steam [°F], respectively
U	Overall heat transfer coefficient [BTU/(sq.ft.hr.°F)]

U_h, U_v, U_T	Overall heat transfer coefficients for heating zone, vaporizing zone, and whole heat exchanger, respectively [BTU/(sq.ft.hr.°F)]
v, V	Axial mean velocity [ft./hr.] and linear velocity of gas in empty tower [ft./sec.], respectively
V_c^n, V_c	Catalyst volume per unit compartment, and of total reactor, respectively [cu.ft.]
W	Quenching water. The subscript denotes the stage number [lb/hr]
$w, \bar{w}$	Parameter subject to variation and that at a specific value considered, respectively
W_R, W_S	Weight of reactor [lb.], mass flow rate of gas in shell side [lb./hr.] respectively
W_{ST}, W_T	Mass flow rate of steam and water in tube side, respectively [lb./hr.]
X, X_e	Fractional conversion of CO at anytime and at equilibrium, respectively. The subscript denotes the stage number and the superscript represents the status.
$\bar{Y}_N$	State vector in N-th stage
Z	Height of packing [ft.]

GREEK LETTERS

ε	Voidage of catalyst bed
$\bar{\theta}_N$	Decision vector at N-th stage
η_1	Effectiveness factor at 1 atm
ζ	Internal porosity of catalyst
λ	Latent heat of water [BTU/lb.]
μ, μ_w	Viscosity of gas and water, respectively [lb./(ft.hr.)]
μ_o	Viscosity of water at tube-wall temperature [lb/(ft.hr.)]
$\varrho, \varrho_m, \varrho_p, \varrho_w$	Density of gas reactor material, catalyst particle, and water, respectively [lb./cu.ft.]
Φ_1	Thiele modulus at 1 atm

APPENDIX

In case that the vaporization is taking place inside the tube, the calculation of heat transfer coefficient is difficult. However, the following simplified approach is used in this study, by separating the heat exchanger fictitiously into two zones: heating zone and vaporizing zone. Then the temperature T_m at which the vaporization starts to take place corresponding to the boundary of the two zones in the tube can be calculated by a heat balance:

$$T_m = T_1 + W_T C_p' (t_2-t_1)/(W_s C_p) \tag{47}$$

The log-mean temperature differences in the heating zone and vaporization zone are:

$$T^1_{l.m.} = [(T_m-t_2)-(T_1-t_1)]/\ln [(T_m-t_2)/(T_1-t_1)] \tag{48}$$

$$T^2_{l.m.} = [(T_2-t_2)-(T_m-t_2)]/\ln [(T_2-t_2)/(T_m-T_2)] \tag{49}$$

The overall heat transfer coefficient for each zone can be obtained by

$$1/U = 1/h_i + 1/h_o + R_d \tag{50}$$

Then the heat transfer areas for heating zone and vaporization zone become

$$A_h = W_T C_p' (t_2-t_1)/(U_h T^1_{l.m.}) \tag{51}$$

$$A_v = 0.5\lambda W_T/(U_v T^1_{l.m.}) \tag{52}$$

Thus the total area is

$$A_T = A_h + A_v \tag{53}$$

And the average overall heat transfer coefficient U_T is obtained

$$U_T = Q/(A_T T^o_{l.m.}) \tag{54}$$

where

$$T^o_{l.m.} = [(T_2-t_2)-(T_1-t_1)]/\ln [(T_2-t_2)/(T_1-t_1)] \tag{55}$$

REFERENCES

[1] ASME Boiler and Pressure Vessel Code, Section VIII, Unfired Pressure Vessels, The American Society of Mechanical Engineers, New York, 1956.
[2] Bellman, R., "Dynamic Programming," Princeton University Press, Princeton, N.J., 1957.
[3] Bhavnani, K.H., Chen, K., "Optimization of Time-Dependent Systems by Dynamic Programming," Joint Automatic Control Conference Proceedings, 1966.
[4] Bohlbro, H., Acta Chem. Scand., 15, 502 (1961).
[5] Bohlbro, H., Acta Chem. Scand., 17, 7 (1963).
[6] Chilton, C., "Cost Engineering in the Process Industries," McGraw-Hill, New York, p. 50, 1960.
[7] Communication, Girdler Catalyst, Louisville, Ky., April, 1968.
[8] Ergun, S., Chem. Eng. Progr. 48, 89 (1952).
[9] Gamson, B.W., Chem. Eng. Progr. 47, 19 (1951).
[10] Kern, D. Q., "Process Heat Transfer," McGraw-Hill, New York, 1950.
[11] Laupichler, F. G., Ind. Eng. Chem. 30, 578 (1938).
[12] Levenspiel, O., "Cehmical Reaction Engineering," John Wiley and Sons, Inc., New York, P. 274, 1962.
[13] Mars, P., Chem. Eng. Sci. 14, 375 (1961).
[14] McCabe, W. L. and Smith, J.C., "Unit Operations of Chemical Engineering," McGraw-Hill, New York, 1956.
[15] Moe, J. M., Chem. Eng. Progr. 58, 33 (1962).
[16] Norman, W. S., "Absorption, Distillation and Cooling Towers," Longmans, England, p. 327, 1961.
[17] Page, J. S., "Estimators' Manual of Equipment and Installation Cost," Gulf, Houston, 1963.
[18] Ruthven, D. M., "The Activity of Commercial Water-Gas Shift Catalysts," Tripartite Conference, Montreal, Sept. 23, 1968.
[19] Ting, A. P. and Wan, S. W., Chem. Eng., May 19, 185 (1969).
[20] Treybal, R. E., "Mass Transfer Operations," Second ed., McGraw-Hill New York, p. 162, 1968.
[21] Utility Gas Production General Accounting Procedure, American Gas Association, May 20, 1965.
[22] Wen, C. Y. and Chang, T. M., Ind. Eng. Chem. Process Design Development 7, 49 (1968).
[23] Wilke, C. R. and Hougen, O. A., Trans. A.I.Ch.E. 41, 445 (1949).